JOURNAL OF MATERIALS SCIENCE **37** (2002) 3509–3514

Wettability of TiC by commercial aluminum alloys

C. A. LEON, V. H. LOPEZ, E. BEDOLLA
Instituto de Investigaciones Metalúrgicas, Universidad Michoacana de San Nicolás de Hidalgo, P.O. Box 52-B, 58000, Morelia, Mich., México
E-mail: ebedolla@zeus.ccu.umich.mx

R. A. L. DREW
Department of Mining and Metallurgical Engineering, McGill University, 3610 University Street, Montreal, QC, Canada, H3A 2B2
E-mail: robin.drew@mcgill.ca

The effect of alloying elements on the wettability of TiC by commercial aluminum alloys (1010, 2024, 6061 and 7075) was investigated at 900°C using a sessile drop technique. Wetting increased in the order 6061 < 7075 < 2024 < 1010 for both, static argon or vacuum atmospheres. Alloys 1010 and 2024 wet TiC under both atmospheres, leading to contact angles in the order of 60° and less, while 7075 only wets under vacuum, with the poorest wettability being exhibited by 6061. Evaporation of Zn and Mg under vacuum conditions contributed to the rupture of the oxide film covering the aluminum drop and thereby improving wetting and spreading. Continuous and isolate Al_4C_3 was detected in all the cases. $CuAl_2$ precipitation at the interface slightly decreased Al_4C_3 formation and increased the adhesion of 2024 to TiC. © *2002 Kluwer Academic Publishers*

1. Introduction

The wetting of molten metals on ceramic surfaces is of crucial importance in liquid state processing of metal-ceramic composites. Though, in general, ceramics are not readily wetted by liquid metals at the usual melt temperatures. Consequently, wettability-enhancing procedures are applied to assist wettability, such as the addition of suitable alloying elements in the melt [1–4]. The composites of the Al/TiC system exhibit attractive mechanical properties for structural applications and can be easily fabricated by capillary melt infiltration [5–8]. It is reported that prior to infiltration an incubation period occurs; a phenomenon partly attributed to the wetting kinetics of the system [6, 7]. Although numerous studies exist concerning the wetting of metal-ceramic systems and its role in the preparation of MMCs [4, 9–11], very little work has been done on the wettability of TiC by aluminum and its alloys.

In the 1970's, Rhee [12] reported that wetting of TiC substrates by aluminum occurs at temperatures above 750°C after 30 min holding time. A non-wetting to wetting transition was found at 1050°C by Kononenko *et al*. [13]. More recently, Muscat *et al*. [6] observed this transition above 860°C; nevertheless, the contact angle did not stabilize even after long holding time, indicating a dynamic wetting behavior. Frumin and coworkers [14] found that by decreasing the value of x of substoichiometric TiC_x compositions, a non-wetting to wetting transition occurred at 800–1100°C, along with the formation of either Al_4C_3 or $TiAl_3$ phases. Such transition observed is found in many other Al/ceramic systems and is commonly associated with the eventual break-up of the oxide film that encapsulates the molten Al drop and prevents the development of a true solid-liquid interface, hence delaying wetting [9, 10, 14]. It is believed that the addition of alloying elements to the melt can influence the disruption of the alumina film, allowing a faster direct metal/ceramic contact [9, 15].

In the present work the wetting behavior of TiC by pure aluminum and three commercial aluminum alloys was investigated using a sessile-drop technique. Contact angles and spreading of the drops were determined as a function of temperature and time in order to establish the effect of the alloying elements on the wetting behavior. Cross sectioned metal/ceramic samples were examined for possible surface reaction products. The results drawn from the present investigation will be valuable in the understanding of the infiltration kinetics of commercial aluminum alloys in TiC preforms previously performed by the authors [7].

2. Experimental

2.1. Substrate preparation

TiC substrates were prepared from c.a.s. grade TiC powder (H. C. Starck, Germany), having a particle size distribution from 0.3 to 3 μm. The chemical composition of the powders is shown in Table I. Dense TiC substrates were obtained by hot pressing 5 g of the as received material in a 2.5 cm diameter graphite die. The conditions were 30 min at 1800°C using a 26 MPa load under ~20 Pa vacuum. The sintered density of the substrates was determined by the Archimedes method (ASTM C 373-88), reaching 96.8%. According to X-ray diffraction, only TiC peaks were observed in the sintered substrates, while SEM examination showed

TABLE I Specifications of the starting TiC powder

Ti	C (total)	C (free)	O	N
79.7%	19.26%	0.1%	0.49%	0.04%

TABLE II Specifications of the alloys used

Alloy	Si	Fe	Cu	Mn	Mg	Cr	Ni	Zn	Ti
Al-1010	0.20	0.65	0.005	0.002	0.014	0.012	0.009	0.002	–
Al-2024	0.35	0.36	4.46	1.08	1.86	0.017	–	0.047	–
Al-6061	0.61	0.40	0.25	0.06	0.82	0.18	<0.009	0.07	–
Al-7075	0.25	0.60	2.21	0.26	2.32	0.22	–	5.52	0.03

that the residual porosity was comprised of closed pores of <1 μm. In principle, the contact angle needs to be measured on smooth surfaces; therefore, the discs were polished to a mirror like finish with 1 μm diamond paste. Roughness measurements performed by atomic force microscopy (AFM) revealed mean roughness values, R_a, from 2.12 to 2.76 nm only. The surface roughness factor, R_w, defined as the ratio of the true to apparent surfaces areas, was 0.032%. Therefore, hysteresis of the contact angle caused by roughness was minimized.

2.2. Contact angle measurement

Wetting experiments were carried out using a sessile drop technique. The experimental equipment consists of a quartz tube furnace, designed specifically for sessile drop tests (Fig. 1), connected to a high vacuum system operating at an absolute pressure of 10^{-4} to 10^{-5} torr throughout the test. The tests were performed at 900°C for all the alloys under vacuum and argon atmospheres. For vacuum operation, the local O_2 partial pressure was reduced by flushing argon and placing a Ti sponge getter in the vicinity of the hot zone. For wetting experiments in argon, the system was first evacuated and then backfilled with ultra-high purity argon (99.999% min) to 0.35 kPa.

Table II shows the specification for the aluminum (1010) and the alloys (2024, 6061 and 7075) used. Metal samples were cleaned in hydrofluoric acid and then in acetone prior to testing. Approximately 0.8 g of metal was placed on the TiC substrates in the furnace before heating. Once the desired temperature was stabilized, the Al-alloy/TiC assembly was pushed into the tube hot zone. At the time the metal drop was well shaped, contact-angle changes with time were followed until a steady state was reached and changes in θ were not appreciable. The contact angle and spreading radius were recorded photographically at various time intervals and accuracy measured directly from the image of the drop section using computational tools. After completion of the experiment, the samples were immediately removed from the hot zone inducing fast cooling. The metal-ceramic interfaces were analyzed by electron probe microanalysis (EPMA) equipped with wavelength dispersive spectroscopy facilities (WDS) for quantitative compositional analysis. The SEM was used either in the secondary electron (SE) or backscattered electron (BE) modes. Both EPMA and SEM were conducted at an accelerating voltage of 15 keV. Conducting X-ray mapping and line-scan distribution of the elements present, as well as quantitative microanalysis for phase identification, made possible direct correlations between structure and composition.

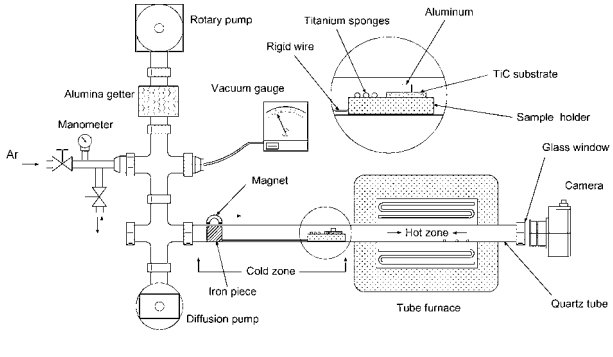

Figure 1 Schematics of the sessile drop apparatus.

3. Results and discussion

3.1. Wettability of TiC by Al and Al-alloys

The variation of the contact angle of the Al-alloys used and TiC are shown in Fig. 2. Generally speaking, the wetting increased in the order 6061 < 7075 < 2024 < 1010 for both vacuum and argon atmospheres. Wetting of pure aluminum on TiC occurred at 900°C with a contact angle lower than 60° after equilibrium was reached. These results do not differ significantly from the values reported by Muscat and Drew [6]. However, Kononenko [13] and Frumin [14] reported a non wetting to wetting transition at ∼1050°C. Because wetting conditions were attained at 900°C, it is suggested that the temperature for wetting transition in the Al/TiC system must be lower than that proposed by Kononenko [13] and Frumin [14], being probably lower than 900°C.

The effect of atmosphere on the wetting behavior was most evident for the 6061 and 7075 alloys, with 6061 exhibiting the slowest spreading kinetics. When testing these alloys under vacuum conditions, evaporation of alloying elements was observed; i.e., after few seconds, a metallic film was deposited in the wall of the quartz tube, mostly near to the cooler parts of the tube. While the 6061 alloy showed a very small variation of θ with time, the contact angle of the 7075 decreased slowly at a nearly constant rate of ∼0.01°/s until reaching a wetting angle close to the equilibrium θ values of 1010 and 2024. The effect of the vapor pressure and the continuous evaporation of the low boiling point elements Zn (907°C) and Mg (1120°C) decreased to some extent the drop volume. This shifted the balance between surface and interfacial forces from one to another with the consequent pulsation of the contact angle at the triple junction. Hence a fluctuating behavior of the wetting curves for the 6061 and 7075 alloys in vacuum were observed (Fig. 2b). The experiments were performed at least three times, thus while the wetting profiles of the 1010 and 2024 alloys showed a smooth change in the curve with a contact angle variation of ±4° as a function of time, the fluctuating curves showed variations among experiments up to ±10°. Even that, the

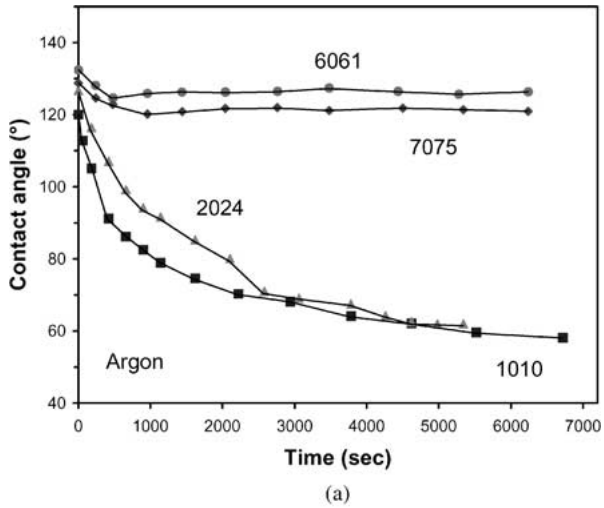

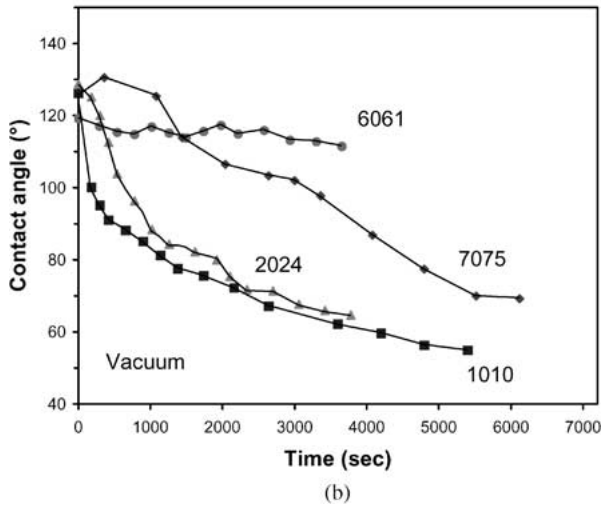

Figure 2 Wettability of TiC by Al-alloys under argon (a) and vacuum (b) at 900°C.

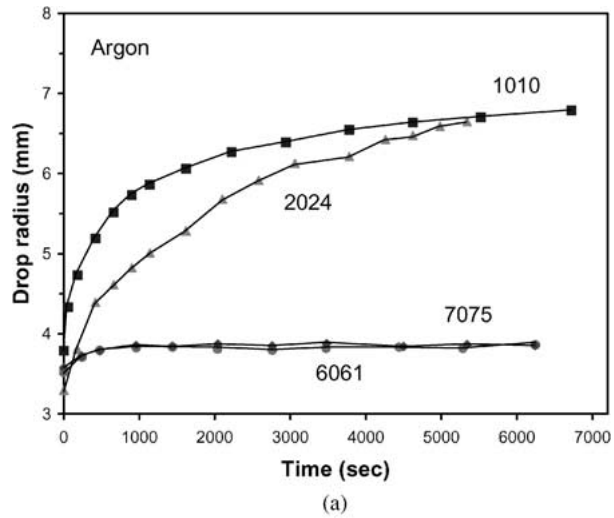

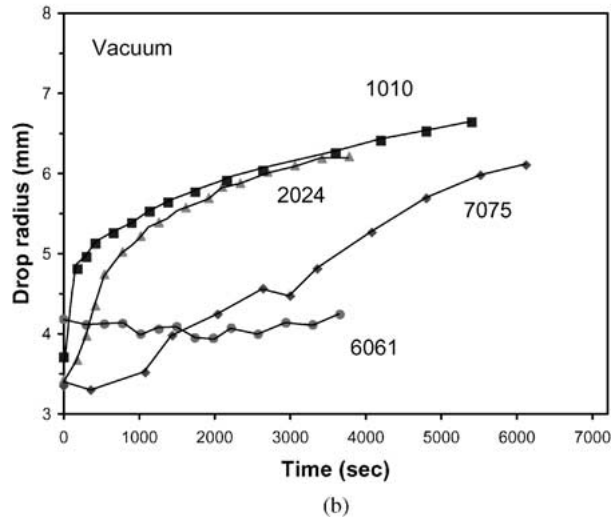

Figure 3 Spreading of Al-alloys on TiC; (a) argon and (b) vacuum.

equilibrium contact angle was always approximately the same.

A different behavior was observed when the 6061 and 7075 alloys, were tested under an argon atmosphere. After an initial slight decrease of θ, the contact angles remained nearly constant for 2 h and steady-state values greater than 118° were obtained for both alloys. The use of argon certainly minimized evaporation of the alloying elements from the drop. However, the chemical composition of the alloys might still be changing with time, since it has been observed that during the fabrication of Al-alloy/TiC composites by melt infiltration, evaporation of the alloying elements occurs above 900°C even at atmospheric pressure [7].

The wetting curves of 1010 and 2024 exhibited a characteristic behavior of non-equilibrium systems, showing a sharp decrease of θ in the first seconds followed by a transition region before a steady-state was achieved. The main changes in θ took place within the first 10 min, so that the contact angle of pure aluminum decreased at a rate of 3.4°/min compared to 2.7°/min for the 2024 alloy in argon. Even though the wetting curves of pure aluminum were similar irrespective of the atmosphere, a slightly lower constant θ was observed under vacuum conditions. This is attributed to the more stable oxide film retained in argon with the consequent delay in spreading of the drop. When the liquid alloy is plainly in contact with the surface of TiC, spreading is driven solely by chemical reaction at the interface [6], which reduces the interfacial tension. Thus, the decrease of the contact angle is proportional to the rate of chemical reaction, which is slightly influenced by the presence of the alloying elements.

Because the spreading kinetics of 1010 was faster than the alloys, the contact angle rapidly approached the steady state value. The behavior of the drop radius curves shown in Fig. 3 suggests that the alloying elements modify the nature of the oxide layer on the drop, thus evaporation becomes a more complex process which results in delayed spreading. Eustathopoulos [15] suggested that only those alloying elements affecting the compactness of the oxide layer have a significant effect on the contact angle. It is known that Mg improves wettability because its rapid evaporation under vacuum damages the alumina film protecting the metal drop. Thus, in the present experiments, the high Mg content in the 2024 and 7075 alloys could lead to the improved wetting behavior under vacuum. It is reported that during the wetting of alumina by a 2.5% Mg containing Al alloy, magnesium volatilized completely at 700°C after 3 min following melting, thus improving wettability [16]. On the other hand, Mg is also highly

TABLE III Possible phases formed by EDX analysis

Composition (at.%)			
Al	C	Ti	Estimated phase
56.5	42.2	1.0	Al_4C_3
25.7	47.9	26.4	$AlTiC_2$
50.8	39.4	9.6	Al_5TiC_4

reactive, and the free energy of formation of its oxide is more negative than that of the oxides of aluminum. This suggests that Mg reduces the aluminum oxide rupturing the oxide film sufficiently to facilitate diffusion and wetting. It is reported that spinel ($MgAl_2O_4$) occurs at low magnesium contents while MgO forms by direct contact with Al-Mg eutectic [17].

Evaporation of the alloying elements contained in 6061 and 7075 alloys decreased in argon, increasing the tenacity of the oxide layer due to their incorporation into the film [15]. This led to a stable and compacted layer containing complex oxides which are more stable under the processing conditions. This film is difficult to break up even after extended periods of time hence, delaying wetting. Results on the evaporation of commercial aluminum alloys have been reported using thermogravimetric analyses in the processing of Al/TiC composites by the current authors [7]. In the case of vacuum conditions, the sudden and violent evaporation of Zn (7075) and Mg (2024), assisted the initial disruption of the surface oxide. Evaporation from the 6061 was more gradual and less excessive, probably because of the lower Mg content (0.82%) in this alloy. However because the equilibrium oxygen partial pressure for aluminum oxidation is exceedingly low, the drop surface was likely covered by a layer of adsorbed gas molecules even under vacuum conditions, thus partially hindering spreading.

3.2. Interface characterization

The dynamic contact angles observed imply that chemical reactions occurred at the alloy/TiC interfaces. By EDX microanalyses it was estimated the exact stoichiometry of the Al_4C_3 compound at the interface in all the specimens in different amounts. This carbide was mainly present in the pure Al/TiC system, where it was found both, as a continuous layer or isolated islands, in some regions up to 6–7 μm in thickness. Even that, because of the reduce volume of the interface, it was not possible to examine accurately cross-section samples of the metal-ceramic couples by XRD, so that no phases other than Al or TiC where identified by this technique. However, similarly than for Al_4C_3, EDX results showed the interfacial formation of other Ti-Al-C compounds in the 1010/TiC and 7075/TiC couples, which best fits the formation of $AlTiC_2$ and Al_5TiC_4, respectively (Table III). Other forms of Al_xC_y carbides, with Al-C ratios different to the best-known Al_4C_3 compound, were occasionally detected throughout the interfaces.

According to the literature, wetting of TiC by aluminum can lead to either clean Al/TiC interfaces [12] or the formation of Al_4C_3 and Al_3Ti compounds

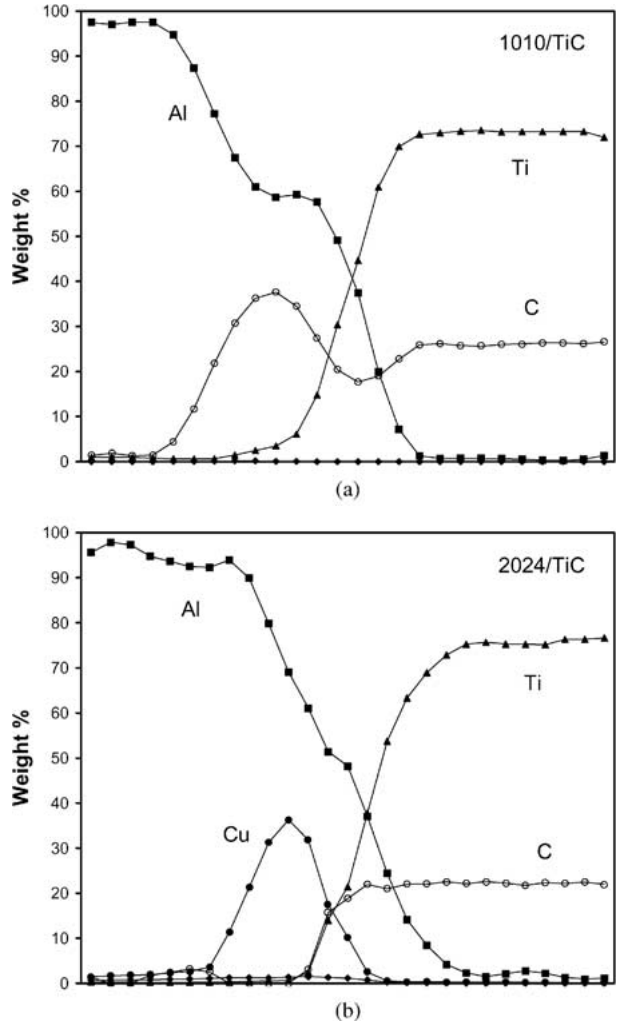

Figure 4 Al/TiC interfaces. (a) Al-1010, (b) Al-2024, (c) Al-6061 and (d) Al-7075.

[14]. While for infiltrated Al/TiC composites, the formation of the complex Ti_3AlC compound [7] has been noted. However, besides the above mentioned compounds and some eutectic and intermetallic phases such as $CuAl_2$ and $MgAl_2$, no other compound was identified in the samples.

Fig. 4 shows typical interfaces found in samples tested under vacuum. The upper gray phase corresponds to the alloys and the lower and light phase is TiC. All the samples present interfacial reaction products. The ceramic surface initially flat and smooth appears rougher because of the dissociation of TiC leading to the formation of Al_4C_3. The thickness of the reaction layer varied within the samples and was discontinuous in nature, particularly for the 7075/TiC and 6061/TiC systems, which exhibited poor wetting in comparison with 1010 and 2024. Intermetallic phases and eutectic zones were observed close to the interface in the 2024/TiC and 7075/TiC samples but only very small amounts of these phases were observed in the case of 6061/TiC.

Examination of drop sections showed that the precipitation of alloyed phases in the ceramic surface decreases the amount of the undesirable Al_4C_3 at the metal/ceramic interface. When the chemical reaction takes place at the solid/liquid interface, TiC dissociates and Al_4C_3 forms. According to the elemental X-ray line-scanning pattern of the 1010/TiC specimen shown

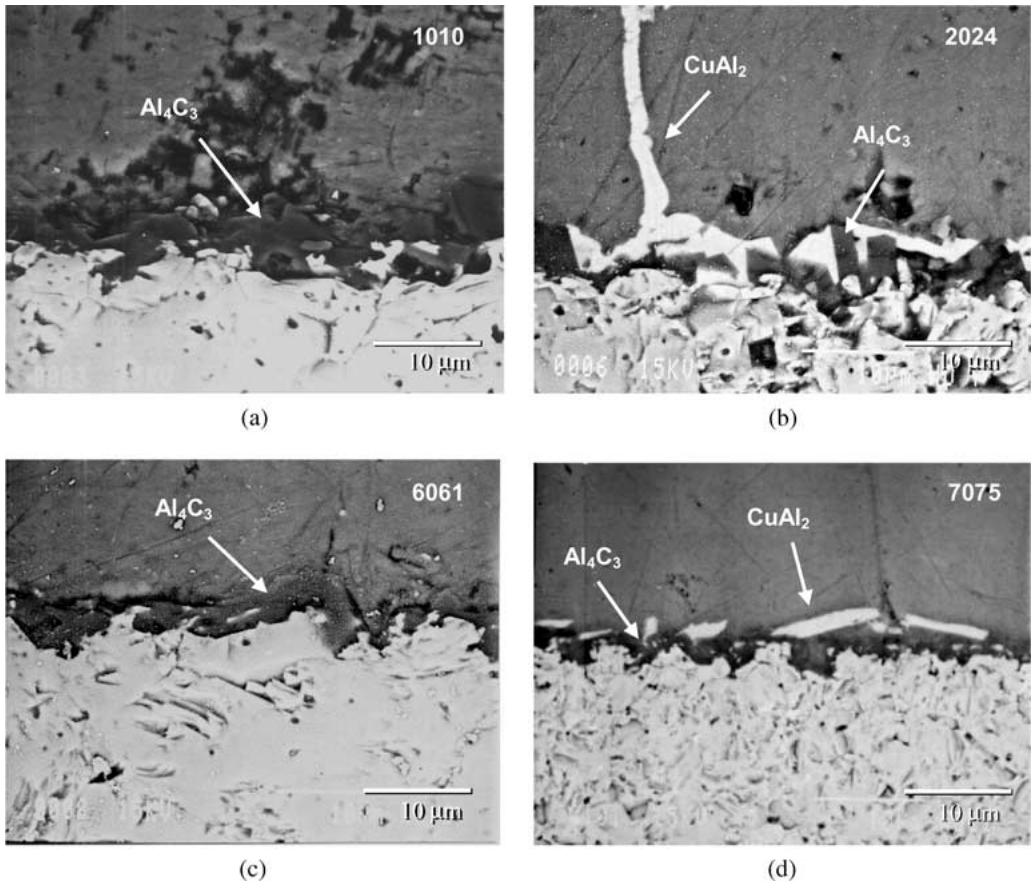

Figure 5 EPMA line-scanning profiles Al-1010/TiC (a) and Al-2024/TiC (b) interfaces. Distance between steps is 1 μm.

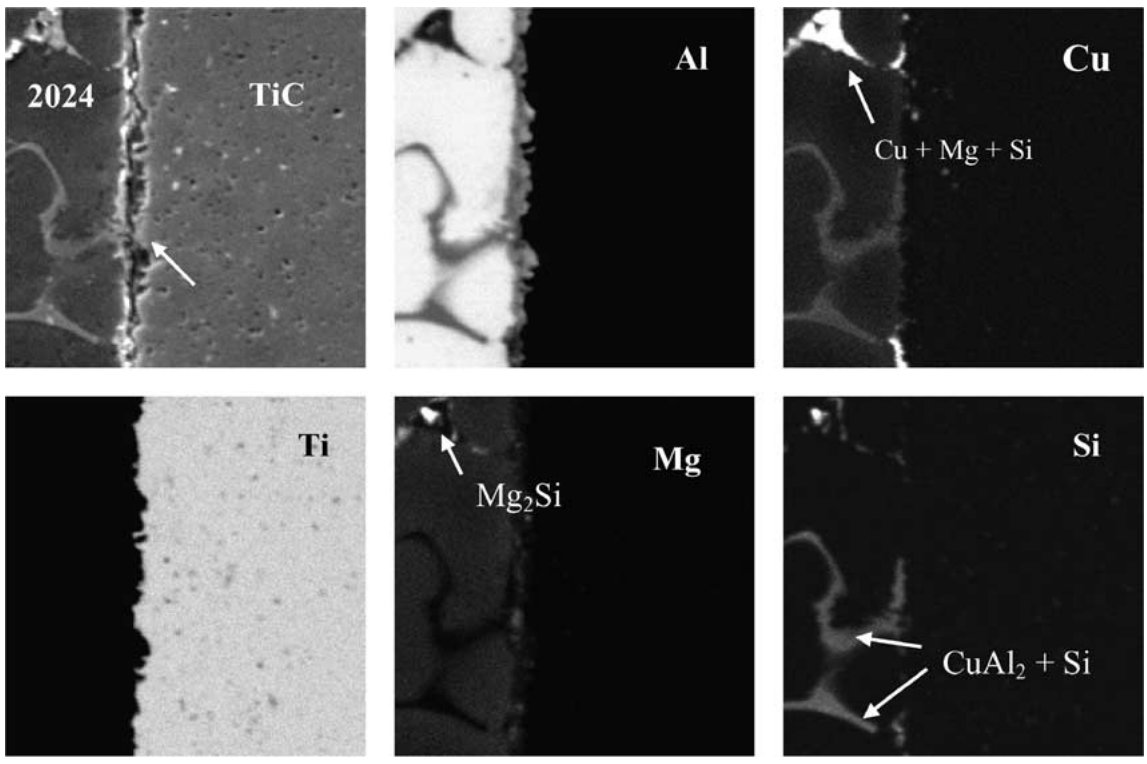

Figure 6 X-ray mapping of a 2024/TiC interface at 900°C under argon.

in Fig. 5a, Ti seems to have formed a complex compound with C and Al adjacent to the substrate in addition to Al_4C_3. However, no traces of Ti were identified in the aluminum nor was the presence of Al_3Ti or any other titanium aluminide observed. The line profile of a 2024/TiC sample in Fig. 5b reveals the formation of an Al-C compound (probably Al_4C_3), while $CuAl_2$ intermetallic is confirmed adjacent to the reaction layer as a result of solidification. As magnesium does not form magnesium carbide, no reaction-aided wetting at the

interface involving magnesium occurred. However, the precipitation of $CuAl_2$ and Mg_2Si was usually observed at the interface.

Elemental mappings by EDX indicated the presence of a reaction layer and precipitates adjacent to the 2024/TiC interface as shown in Fig. 6. These intermetallics are mostly $CuAl_2$ and Mg_2Si and free Si. Al_4C_3 is formed due to the reaction and partial dissolution of TiC in liquid Al that takes place during the wetting process. This mode of interaction and the increasing copper content at the interface can prevent the formation of Al_4C_3. Froumin *et al*. [18] report that in the presence of TiC, alloying with Cu decreases the solubility of Ti in molten Al. Hence this reduces the amount of titanium being transferred into the melt and thereby lowering wetting of the drop. The work of adhesion of the 1010/TiC and 2024/TiC systems, calculated from the surface tension data given by Orkasov [19] and contact angle values corresponding to 1 h holding time, indicate that adhesion was slightly higher under vacuum conditions, particularly for the 2024 alloy. The values obtained were 1190 mJ/m^2 and 1224 mJ/m^2 for 1010, and 1207 mJ/m^2 and 1254 mJ/m^2 for 2024 under argon and vacuum conditions, respectively. This can be explained on the basis of the drop being less oxidized but, above all, it indicates the contribution of the copper precipitates near to the interface on the energy of adhesion.

On the basis of the current findings, alloying elements do not improve the wetting of Al on TiC through interfacial chemical reaction. However, it appears that the precipitation of intermetallic phases delays the formation of Al_4C_3. The alloy that showed the best wetting behavior was 2024, where the main alloying elements are Cu and Mg. It is concluded that multi-component alloys cause conflicting effects on wetting. Therefore, the authors are currently investigating experiments involving binary and ternary alloys.

4. Conclusions

1. Wettability of TiC by molten aluminum and its alloys increased in the order $6061 < 7075 < 2024 < 1010$. Good wetting was observed for 1010 and 2024 with steady contact angles close to 60°. The 7075 alloy wets TiC only under vacuum, with the 6061 exhibiting the poorest wettability.

2. Excessive evaporation of the low boiling point Zn and Mg alloying elements was observed under vacuum conditions. This contributed to the rupture of the oxide film covering the aluminum drop and thereby improving wetting and spreading. The argon atmosphere reduced the evaporation and the extent of wetting of 6061 and 7075 alloys. Pure aluminum and 2024 showed minimum sensitivity to the atmosphere.

3. Wetting behavior found in Al-alloys/TiC systems is typical of reactive systems. Interface examination revealed the formation of Al_4C_3 in all the cases; the thickness of the reaction layer varied within the samples and was discontinuous in nature, particularly for the 7075/TiC and 6061/TiC systems, which exhibited poor wetting.

4. Copper precipitates close to the interface were mainly observed in 2024 and 7075 alloys. Generally speaking, their presence led to a reduction in the formation of Al_4C_3 and an increase in the adhesion of 2024 to TiC. As magnesium has no tendency to form carbides, this element took no part in reaction-aided wetting. However, the formation of some Mg_2Si along with $CuAl_2$ was observed.

Acknowledgements

The authors acknowledge the financial support of the National Council for Science and Technology of Mexico (CONACYT, grant 25702-A), Coordinación de la Investigación Científica (Universidad Michoacana, Mexico) and the Natural Sciences and Engineering Research Council of Canada (NSERC). We also thank the technical assistance of J. Lemus and G. Poirier from McGill University in the hot pressing and EPMA analysis of the samples.

References

1. R. ASTHANA and S. N. TEWARI, *Compos. Manuf.* **4** (1993) 3.
2. F. DELANNAY, L. FROYEN and A. DERUYTTERE, *J. Mater. Sci*. **22** (1987) 1.
3. A. BANERJI, J. K. ROHATGI and W. REIF, *Metall. Tech*. **38** (1984) 656.
4. R. ASTHANA, *J. Mater. Sci*. **33** (1998) 1959.
5. D. MUSCAT and R. A. L. DREW, *J. Mater. Sci. Technol*. **8** (1992) 971.
6. *Idem*., *Metall. Trans*. **25A** (1994) 2357.
7. A. CONTRERAS, M. SALAZAR, E. BEDOLLA, C. A. LEON and R. A. L. DREW, *Mat. Manuf. Process* **15** (2000) 163.
8. A. ALBITER, C. A. LEON, R. A. L. DREW and E. BEDOLLA, *Mater. Sci. Eng*. **289A** (2000) 109.
9. A. C. FERRO and B. DERBY, *Acta Metall. Mater*. **43** (1995) 3061.
10. V. LAURENT, D. CHATAIN, C. CHATILLON and N. EUSTATHOPOULOS, *ibid*. **36** (1998) 1797.
11. H. MIYAHARA, R. MUROAKA, N. MORI and K. OGI, *J. Japan Inst. Metals* **59** (1995) 660.
12. S. K. RHEE, *J. Amer. Ceram. Soc*. **53** (1970) 386.
13. V. Y. KONONENKO, G. P. SHVEJKIN, A. L. SUKHMAN, V. I. LOMOTSEV and B. V. MITROFANOV, *Poroshk. Metall*. **9** (1976) 48.
14. N. FROUMIN, N. FRAGE, M. POLAK and M. P. DARIEL, *Scripta Metal*. **37** (1997) 1263.
15. N. EUSTHATOPOULOS, J. C. JOUD, P. DESRE and J. M. HICTER, *J. Mater Sci*. **9** (1974) 1233.
16. Z. LIJUN, W. JINBO, Q. JITING and N. OIU, in "Interfaces in Metal-Ceramics Composites," edited by R. Y. Lin *et al*. (TMS, Warrendale, PA, 1989) p. 213.
17. R. N. LUMLEY, T. B. SERCOMBE and G. B. SCHAFFER, *Metall. Mater. Trans*. **30A** (1999) 457.
18. N. FROUMIN, N. FRAGE, M. POLAK and M. P. DARIEL, *Scripta Metal*. **48** (2000) 1435.
19. T. A. ORKASOV, *High Temperature*, **34** (1996) 490.

Received 17 May 2001
and accepted 9 April 2002